

Optimization of plated steel beams using metamodels and modern optimization methods

A. Šťastný^{a,*}

^a*Institute of Automotive Engineering, Department of Handling and Building Machines, Faculty of Mechanical Engineering, Brno University of Technology, Technická 2896/2, 616 69 Brno, Czech Republic*

Received 22 February 2015; received in revised form 22 April 2015

Abstract

This paper deals with metamodel-based optimization of plated steel beams. The first part of the article explains the principle of the metamodel-based optimization approach and also provides basic information on incorporated sub-methods such as design of experiments (DOE), mathematical approximation methods and mathematical optimization methods. Since optimized sections tend to be slender and thus susceptible to buckling, special attention is paid to the buckling evaluation. Both linear and nonlinear buckling analyses are employed. The nonlinear buckling analysis addresses detrimental influence of imperfections on the limit load by introducing equivalent geometric imperfections into the finite element (FE) model. The shapes and magnitudes of these imperfections are based on recommendations for plated beams given in Eurocode 3 (EC3). The practical part of the article illustrates the approach on step by step basis using an example of spreader beam weight optimization. It is shown that simple metamodels can efficiently substitute the FE model in optimization, thereby making the process very fast. The parametric FE models are developed in the Ansys Parametric Design Language (APDL). The governing algorithm, as well as most of the mathematical sub-methods, is realized in the Matlab software.

© 2015 University of West Bohemia. All rights reserved.

Keywords: optimization, metamodeling, imperfection, buckling, steel beam

1. Introduction

Analyses of engineering structures have undergone considerable changes in the last twenty years. The major changes reflect the development in the field of computational methods, hardware and software. Employment of FEM-based software packages in practical engineering enables solving more complex problems in comparison with the traditional analytical approach. Most of design codes still rely on the analytical approach; however, FEM-based procedures and recommendations have started to appear. For example, annex C of [3] gives practical recommendations on performing FE analyses of plated steel structures.

Both analytical and FEM-based approaches can be adopted in structural optimization, which is a process of identifying the best product parameters with respect to a predefined design goal (or goals) and design constraints. The design goal is expressed as an objective function. The product parameters which can be changed by the designer are called design variables. Assigning each design variable to an axis of the orthogonal coordinate system, we define a multi-dimensional space, which is referred to as design space. Since the range of each design variable is limited to an interval, the design space is limited as well. Design constraints delimit a subset of the design space which is referred to as feasible region. The task of an optimization algorithm is to search for an extreme of the objective function inside the feasible region of the design space. Fig. 1 depicts the principle of optimization.

*Corresponding author. Tel.: +420 776 283 794, e-mail: antonin_stastny@centrum.cz.

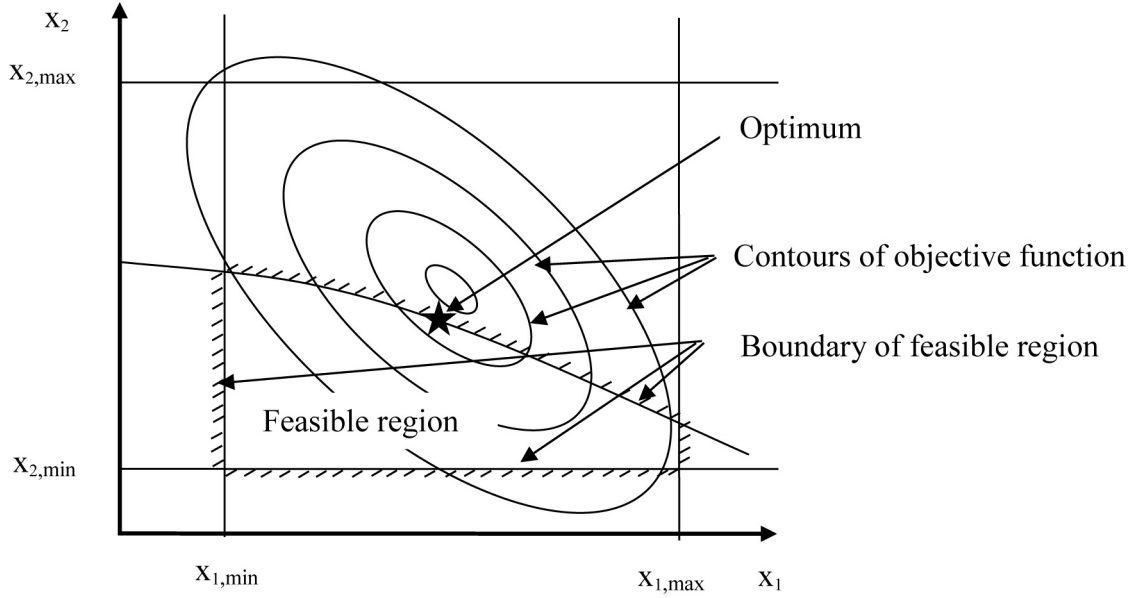


Fig. 1. Principle of optimization

In an optimization problem, design variables are organized in a design vector

$$\mathbf{X} = (x_1, x_2, \dots, x_n)^T, \quad (1)$$

where x_1 through x_n are design variables. The objective function can be expressed as a function of design variables

$$f(\mathbf{X}) = f(x_1, x_2, \dots, x_n). \quad (2)$$

Design constraints are expressed as equalities and inequalities dependent on design variables

$$g_i(\mathbf{X}) = 0 \quad \text{for } i = 1, 2, \dots, m, \quad (3)$$

$$h_j(\mathbf{X}) \leq 0 \quad \text{for } j = 1, 2, \dots, p, \quad (4)$$

$$x_k \in \langle x_{k\min}; x_{k\max} \rangle \quad \text{for } k = 1, 2, \dots, n. \quad (5)$$

Here m is the number of equality constraints, p is the number of inequality constraints and n is the number of design variables. Expression (5) defines the design space.

Optimization is often performed by using the trial and error approach in practical engineering. Despite considerable advances in computing hardware development, each trial can represent a long running FE analysis. Furthermore, trial and error approach does not explain functional relationships between design variables and output quantities. To solve the optimization systematically, mathematical optimization methods have to be adopted. Using the analytical approach to conduct the structural analysis, the objective function and design constraints can be directly expressed as closed-form mathematical functions of design variables; however, this is possible for simple problems only. Complex engineering analyses rely on FEM, which unfortunately does not directly provide closed-form expressions for the objective function and design constraints. To address this drawback of FEM, metamodeling can be used as a possible solution. The flow of the metamodel-based optimization approach is outlined in Fig. 2.

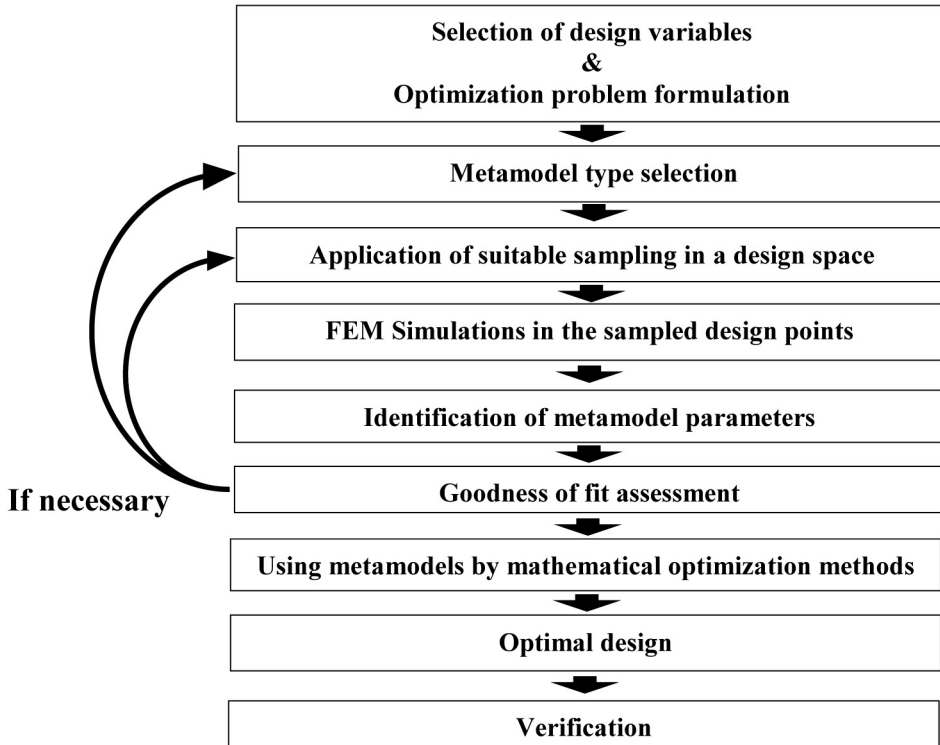


Fig. 2. Principle of metamodel-based optimization

2. Brief overview of key sub-methods of metamodel-based optimization

2.1. Design of experiments (DOE)

As outlined in the Introduction, DOE is a sampling strategy in a design space which is aimed to identify an efficient set of experiments (FE simulations) for acquiring data for identification of metamodels' parameters. Application of this strategy maximizes metamodel quality, even though the number of needed experiments is reduced. DOE sampling plans can be divided into two basic groups:

- **Statistical plans**

These plans are designed especially for physical experiments, i.e. experiments which possess a random error. To eliminate influence of this error on metamodel quality, statistical plans prescribe more replications at one point and some of them also locate sample points on or near boundaries of the design space. These plans are often applied without replications in the field of computer experiments. The most popular statistical plans are: full factorial design (Fig. 3a), partial factorial design, central composite design (Fig. 3b) and Box Behnken design. A detailed description of the statistical plans can be found in [7].

- **Space filling plans**

These plans are intended to be used for computer experiments, i.e. experiments without the random error. In order to explore the response variability, samples are evenly and economically distributed in whole volume of the design space. These plans generate higher number of samples, because the computer experiments are cheaper and faster than the physical ones. These plans are often called modern plans. The most popular modern

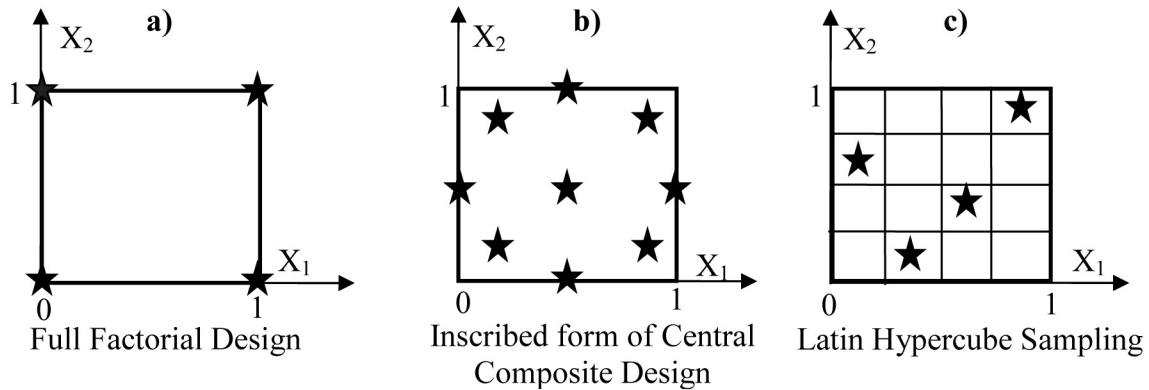


Fig. 3. Examples of 2D experimental designs in unit design space

plans are: Latin hypercube sampling (Fig. 3c), pseudo Monte Carlo sampling, quasi Monte Carlo sampling, maximin and minimax designs. A detailed survey of the modern plans is presented in [6].

2.2. Mathematical approximation methods

Mathematical approximation methods construct approximate descriptions of relationships between design variables and responses of primary models (e.g. FE models). These approximations are often referred to as metamodels. Metamodels are built from a moderate number of experimental data (results of FE analyses in case of computer experiments) in order to provide fast approximate results over the design space or its sub-region. There are many alternative metamodel types. The choice of a particular form primarily depends on the degree of variability of the approximated response. Responses showing linear or slightly nonlinear global trends can be approximated by low order polynomial metamodels. Responses showing higher degree of nonlinearity have to be approximated by more sophisticated methods such as artificial neural networks, radial basis functions or kriging. Since the response quantities used in optimization of steel beams show smooth global trends in their variability, second order polynomials seem to be sufficient. The least square method is used to identify their parameters from a set of experimental data. This method is straightforward and the polynomial objective function and design constraints are easy to use and in design exploration and optimization. The general form of the second order polynomial metamodel can be expressed as

$$\hat{Y}(\mathbf{X}) = \beta_0 + \sum_{i=1}^n \beta_i x_i + \sum_{i=1}^n \beta_{ii} x_i^2 + \sum_{i < j} \sum_{i=1}^n \beta_{ij} x_i x_j, \quad (6)$$

where $\hat{Y}(\mathbf{X})$ is the approximated response (metamodel), \mathbf{X} is the design vector, $\beta_0, \beta_i, \beta_{ii}, \beta_{ij}$ are regression coefficients, x_i is the i^{th} design variable and n is the number of design variables.

Before using a metamodel in optimization, a goodness of fit assessment shall be done. The coefficient of determination is often used as a global measure of approximation quality. This coefficient quantifies how much variability in a response is explained by the metamodel. Its value lies in the interval $(0; 1)$. The bigger value indicates the better quality of approximation. The coefficient of determination is defined by equations (7) through (11).

$$R^2 = \frac{SS_M}{SS_T} = 1 - \frac{SS_E}{SS_T}, \quad (7)$$

$$SS_M = \sum_{i=1}^n (\hat{Y}(\mathbf{X}_i) - \bar{Y})^2, \quad (8)$$

$$SS_T = \sum_{i=1}^n (Y(\mathbf{X}_i) - \bar{Y})^2, \quad (9)$$

$$SS_E = \sum_{i=1}^n (Y(\mathbf{X}_i) - \hat{Y}(\mathbf{X}_i))^2, \quad (10)$$

$$\bar{Y} = \frac{1}{n} \sum_{i=1}^n Y(\mathbf{X}_i). \quad (11)$$

Here, SS_M is the metamodel sum of squares, SS_T is the total sum of squares, SS_E is the residual sum of squares, \mathbf{X}_i is the i^{th} design point, $Y(\mathbf{X}_i)$ is the exact value of the response Y in the i^{th} design point, \bar{Y} is the average value of Y , $\hat{Y}(\mathbf{X}_i)$ is the approximated value of $Y(\mathbf{X}_i)$ in the i^{th} design point, n is the number of design points given by the DOE plan. In addition to R^2 , the following measures can be used to estimate local deviations:

$$MAE = \frac{1}{n} \sum_{i=1}^n (\hat{Y}(\mathbf{X}_i) - Y(\mathbf{X}_i)), \quad (12)$$

$$REL = \max \left| \frac{\hat{Y}(\mathbf{X}_i) - Y(\mathbf{X}_i)}{Y(\mathbf{X}_i)} \right|, \quad (13)$$

$$MAX = \max |\hat{Y}(\mathbf{X}_i) - Y(\mathbf{X}_i)|. \quad (14)$$

Here, MAE is the mean absolute error, REL is the maximum relative error and MAX is the maximum absolute error.

2.3. Mathematical optimization methods

The optimization methods for continuous functions can be divided into three main groups:

- **Differential calculus analytical methods**

These methods are analytical and make use of the differential calculus to find the optimum. The functions have to be twice differentiable with respect to all design variables. According to the form of constraint functions, optimization problems can be solved by direct substitution, Lagrange multiplier method or by application of Kuhn-Tucker optimality conditions. The main advantage of these methods is their analytical nature, i.e. finding an optimum without a troublesome iterative process. The main drawbacks are the differentiability requirement and applicability to simple problems only.

- **Differential calculus numerical methods**

The main idea of this group of methods is based on the fact that the gradient points in the direction of the steepest ascend of a function. Starting the iterative procedure from an initial estimate of an optimal point, the algorithm iteratively approaches the optimum. The following fundamental questions have to be answered at the end of each iteration:

- Is the current point the optimal point?
- In which direction to continue?
- How far to continue?

According to the form of the objective function and design constraints, linear programming, quadratic programming or nonlinear programming algorithms are adopted. Since most optimization problems in engineering result in nonlinear objective functions and/or design constraints, the nonlinear programming algorithms have to be often used. In most cases, these methods converge faster to the optimum point in comparison to heuristic methods. The main drawback is their tendency to find a local optimum.

• Heuristic optimization methods

The fundamental principles of these methods are inspired by natural processes such as natural evolution, behaviour of swarms or ant colonies. Apart from gradient-based methods, the heuristic methods make use of random numbers instead of derivatives to find new optimum candidates. Since these algorithms tend to explore whole volume of the design space, there is high probability to find the global optimum. A drawback of these methods is very high number of functional evaluations in comparison to gradient-based algorithms. On the other hand, this drawback can be substantially reduced by using simple metamodels which are evaluated very quickly.

In majority of engineering problems, selection of a suitable optimization method is restricted by the following facts:

- Inequality design constraints such as stress and deflection limits are always present.
- Objective functions and/or design constraints tend to be nonlinear.

Based on the above mentioned restrictions and capabilities of the Matlab optimization toolbox, the sequential quadratic programming (SQP) is chosen as a representative of gradient-based methods and the genetic algorithm (GA) as a representative of heuristic methods. Both SQP and GA represent the state of the art optimization schemes. Detailed description of both algorithms is beyond the scope of this article and can be found in [8] and [9]. As the objective function and design constraints are second order polynomials, the optimization is expected to be quickly running using both algorithms. It is an advantage to use both gradient-based and heuristic methods, because of mutual verification of results.

3. Consideration of buckling in optimization

Weight optimization of plated beams results in slender sections, which may become unstable (buckle) before strength and deflection criteria are violated during loading. Since buckling can govern the design, it has to be addressed in the optimization problem formulation. There are two basic forms of buckling: *bifurcation buckling* and *limit load buckling* [5].

The bifurcation buckling is a sudden transition from a stiff membrane (axial) dominated equilibrium path to a flexible bending dominated equilibrium path. Although this behaviour is inherent to ideal axially or in-plane loaded structural members, it can be practically regarded as a limiting behaviour of certain types of structural members with vanishingly small imperfections. The load at which the bifurcation takes place is called critical or bifurcation load (see M_{cr} in

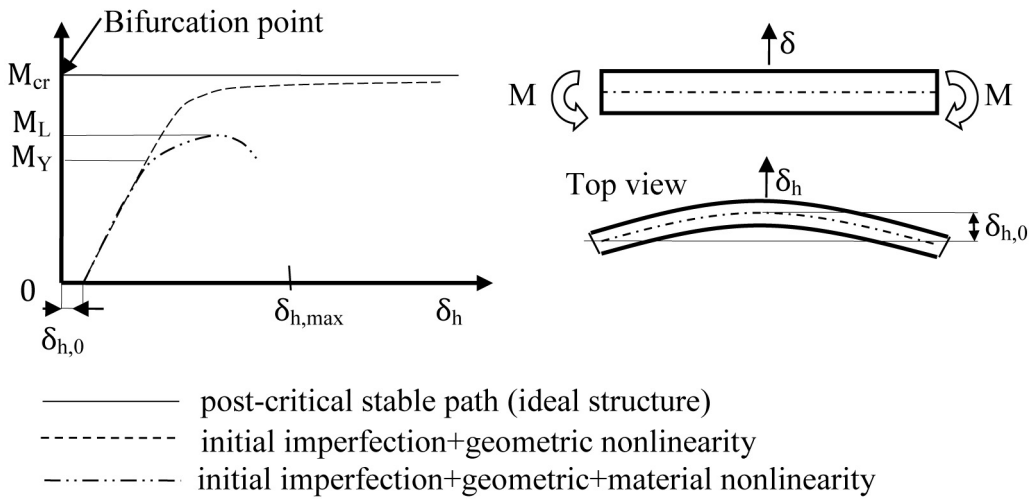


Fig. 4. Critical and limit loads on schematic load-deflection diagrams

Fig. 4). It is well known that the critical load can be a non-conservative estimate of a load at which the structure starts to behave unstably. This can be explained by the unavoidable presence of imperfections, which prevent the structure from reaching the bifurcation point. The deformation field follows the geometrical imperfection pattern from the beginning of loading and beyond a certain level of load the deformations start to grow considerably faster than before. This behaviour represents a loss of overall stiffness and the structure starts to behave unstably. The rapid grow of deformation can be recognized on load-deflection diagrams according to changes in their slope/curvature.

Since the transition between the membrane dominated equilibrium path and the bending dominated path is not sudden, it is not so straightforward to define a load representing the beginning of unstable behaviour. This load is referred to as limit load. The limit load can be defined in several different ways. For example, civil engineers often define the limit load as a load corresponding to the maximum of a load-deformation diagram (see M_L in Fig. 4). Considering elastic-plastic properties of material, the limit load according to this definition indicates development of a plastic hinge. Apart from buildings, loadings on steel structures of mechanical devices such as manipulators or lifting devices are limited by yielding (see M_Y in Fig. 4). It is important to bear in mind that slender beams may become unstable before the yield criterion is violated. This is given by higher sensitivity to geometrical nonlinearity, which can cause large displacements while the material behavior is still elastic. In this case, the design is governed by a deflection constraint. In general engineering practice, this is quite rare, because most of the structures are of intermediate slenderness where yielding takes place before the structure starts to lose stability. The loss of load carrying capacity of such structures is caused by interaction of yielding and buckling.

In case of beams, two basic buckling modes can occur when the critical load is reached. The first mode is local, because only localized compressed areas of webs and/or flanges buckle (see Fig. 5). This mode is referred to as local or plate buckling. The second mode is global, because whole compressed flange deflects laterally. Because of structural compatibility, beam cross sections are also rotated (see Fig. 6). This global mode is referred to as flexural-torsional buckling. The global mode is more dangerous, because locally buckled plates possess considerable post-buckling strength.

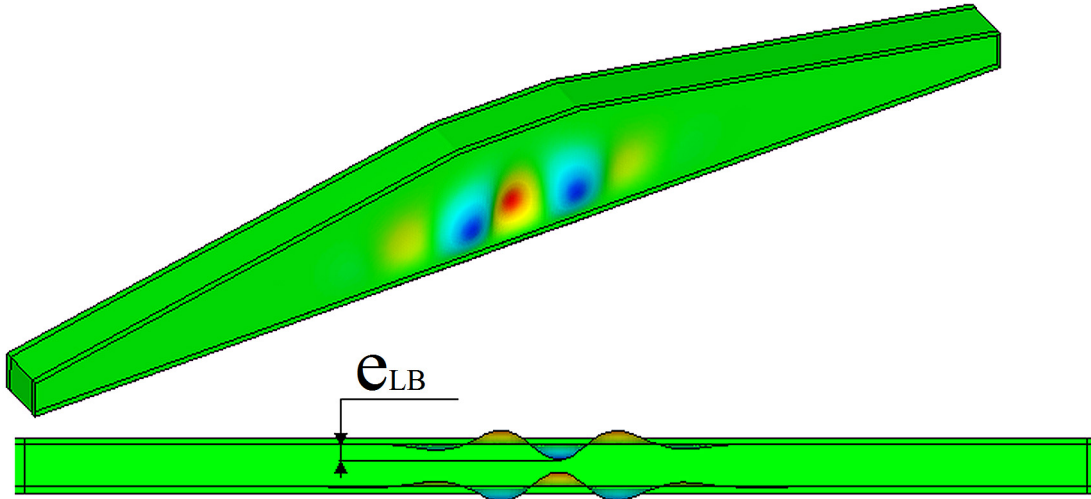


Fig. 5. Local buckling mode

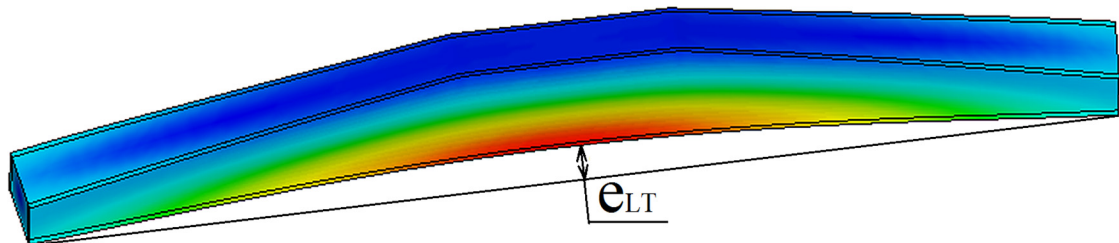


Fig. 6. Lateral-torsional buckling mode

As far as the FEM-based buckling analysis is concerned, there are two general approaches. The linear buckling analysis (LBA) calculates critical load parameters by solving the eigenvalue problem

$$(\mathbf{K} + \lambda \cdot \mathbf{K}_G) \cdot \bar{\mathbf{U}} = \mathbf{0}, \quad (15)$$

where \mathbf{K} is the global stiffness matrix, \mathbf{K}_G is the geometric stiffness matrix, $\bar{\mathbf{U}}$ is the mode shape vector and λ is the critical load parameter. The solution of this problem provides information on both critical loads and corresponding mode shapes. The solution consists of as many critical load parameters and mode shapes as there are degrees of freedom in the FE model. Practically, the lowest critical buckling mode is of interest. Both local and global mode shapes are provided.

The nonlinear buckling analysis with imperfections (GNIA) applies loads incrementally. Depending on application, elastic or elastic-plastic material model can be used. Annex C of [3] gives recommendations on performing the nonlinear buckling analysis of plated structures. It is recommended that the imperfection pattern should be created by an appropriate combination of adequately scaled mode shapes from LBA. It is indicated that a leading imperfection should be chosen and then accompanying imperfections may have their values reduced to 70 % of the full values. Table C.2 of [3] provides amplitudes of equivalent geometrical imperfections, which are based on correlation with practical tests and thus account for the influence of residual stresses as well. The main problem for an engineer is to choose which combination of imperfections is critical. Since the global load carrying behaviour is of interest, the global lateral-torsional mode is chosen as the leading and the first local buckling mode as the accompanying imperfection.

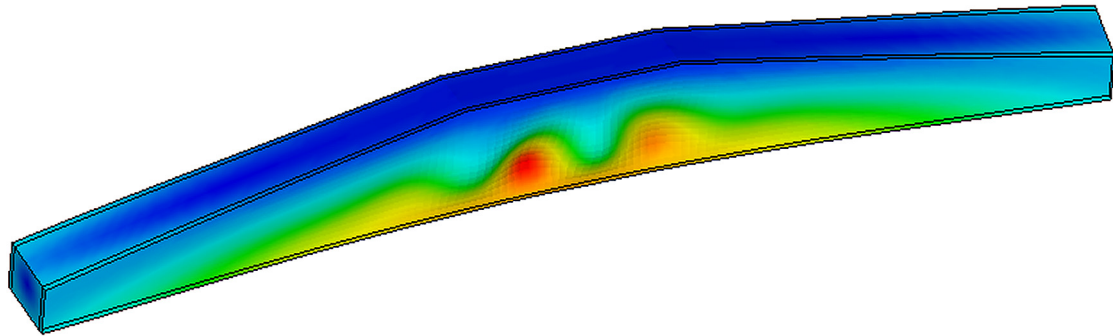


Fig. 7. Combined imperfection

Introducing a combination of both global and local modes allows for an interaction effect of these two modes. This is important, because global failures can be initiated by local ones. The combined imperfection is depicted in Fig. 7.

4. Case study

In this section, the metamodel-based optimization methodology is applied to the weight optimization of a spreader beam depicted in Fig. 8. In general, more than eight design variables can be defined. In order to graphically illustrate the process, the problem is reduced to two design variables only. This reduction enables better visualization of the objective function and design constraints by means of 3D plots. For comparison, three conceptually different DOE plans are generated. Subsequently, a series of FE analyses is performed and parameters of second order polynomial metamodels are identified. These metamodels are directly used as the objective function and design constraints in the optimization process. A parametric FE model is developed in APDL. Matlab software is used for DOE, metamodel identification and optimization. Whole process is automatized and driven from Matlab.

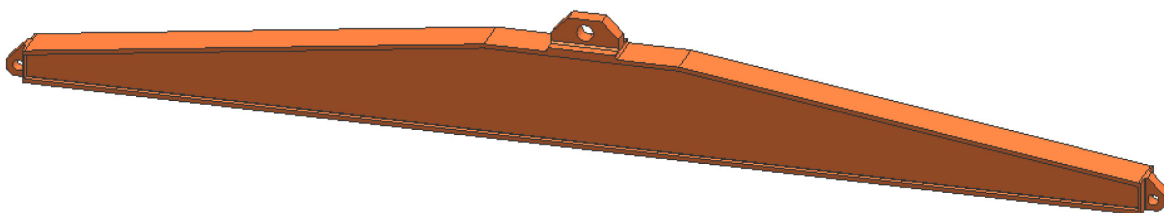


Fig. 8. Spreader beam

4.1. Optimization problem description

The goal of this optimization problem is to find a lightweight configuration of a pre-designed spreader beam (see Fig. 8) by finding optimal thicknesses of flanges and webs. The working load limit (WLL) is 20 tons and the span of lifting hinges is 4 m. The beam will not experience more than 10 000 loading cycles during its design life. The strength requirements given in harmonized standard [1] shall be fulfilled. The beam is produced from structural steel S355 J2G3. The mechanical and physical properties are taken from [2] as follows: the yield stress $f_y = 355$ MPa, the Young's modulus $E = 210\,000$ MPa and the Poisson's ratio $\mu = 0.3$.

Fig. 9 shows design parameters of the spreader beam. In our case, parameters tf and tw are design variables and the remaining design parameters are kept at their pre-designed values, which are listed in Table 1.

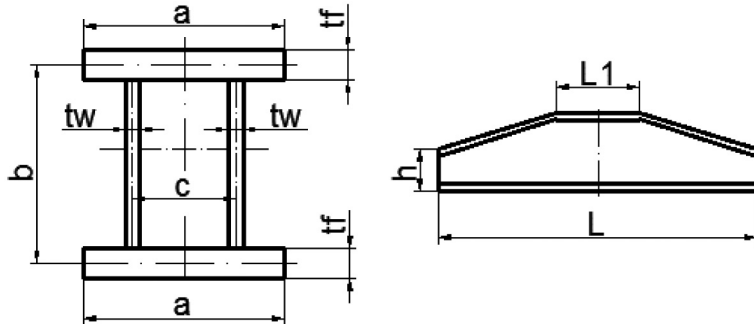


Fig. 9. Parameters of spreader beam

Table 1. Design parameters

| parameter | value [mm] | parameter | value [mm] | parameter | value [mm] |
|-----------|------------|-----------|------------|-----------|------------|
| a | 250 | tf | 6–10 | $L1$ | 800 |
| c | 210 | tw | 4–6 | h | 200 |
| b | 500 | L | 4 000 | | |

4.2. Design criteria

Standard [1] defines a load case

$$X = S_{DL} + 2 \cdot S_{WLL}, \quad (16)$$

where S_{DL} represents a self-weight of attachments and S_{WLL} is the work load limit. The coefficient “2” plays a role of a safety factor, which also accounts for the dynamic effect of lifting and static test. The self-weight of attachments is considered negligible in comparison to $S_{WLL} = 20$ t.

The structure shall fulfil the following design criteria for the load case (16):

- a) The Von Mises stress in plates shall not exceed the yield stress.
- b) The beam shall not buckle. Both lateral-torsional and plate buckling shall be taken into account.

The standard also ensures that beams fulfilling its criteria can experience up to 20 000 loading cycles without a special fatigue check. Deflection limits are not specified in the standard; however, it is convenient to specify a limit on vertical deflection to ensure reasonable stiffness. Please note, that vertical deflection is evaluated for the work load limit of 20 tons.

- c) The vertical deflection shall not exceed $L/500$.

4.3. Mathematical formulation of the optimization problem

The optimization problem is defined by an objective function and five inequality design constraints. The design constraints are formulated according to the limits a–c described in section 4.2. The design variables creates a design vector

$$\mathbf{X} = (tf, tw)^T, \quad (17)$$

where tf is the flange thickness and tw is the web thickness.

- Objective function: beam volume [mm³]

The beam volume is taken directly from the FE model in each design point.

$$\text{Volume} = \text{Volume}(\mathbf{X}) [\text{mm}^3], \quad (18)$$

- Design constraint 1: Von Mises stress shall not exceed the yield stress.

$$\sigma_{EQV} \leq f_y [\text{MPa}], \quad (19)$$

where σ_{EQV} is the Von Mises equivalent stress, f_y is the yield stress.

- Design constraint 2: Buckling safety factor shall be greater or equal to 1.

$$k_B \geq 1 [-], \quad (20)$$

where k_B is the buckling safety factor. As explained in [4], the lowest critical load parameter from LBA shall be considered along with the limit load.

- Design constraint 3: Vertical deflection shall not exceed $L/500$ mm.

$$\delta \leq L/500 [\text{mm}], \quad (21)$$

where δ is the vertical deflection and L is the beam length.

- Design constraint 4: Flange thickness shall be within the interval ⟨6 mm; 10 mm⟩.

$$6 \leq tf \leq 10 [\text{mm}], \quad (22)$$

where tf is the flange thickness.

- Design constraint 5: Web thickness shall be within the interval ⟨4 mm; 6 mm⟩.

$$4 \leq tw \leq 6 [\text{mm}], \quad (23)$$

where tw is the web thickness.

Design constraints 4 and 5 define the two-dimensional design space.

4.4. Finite element model

The parametric FE model is developed in APDL. Ansys Shell 181 elements are used for this application, because they are suitable for modelling thin to moderately thick plate and shell structures transmitting membrane and bending actions. Since the thickness is a parameter of shell 181 elements, the FE mesh does not change among all evaluated configurations. The element size has been established by performing a mesh sensitivity study. Loads are transmitted to the structure by surface-based constraints realized by the multi-point constraint (MPC) contact algorithm. The boundary conditions are applied so that they simulate the real situation, i.e. freely hanging beam. Special attention is paid to enable development of the lateral-torsional mode of buckling. In order to enable lateral displacement of the hook location (application point of the force F) and also to prevent beam rotation about the longitudinal axis, a weak spring element is used. Since the stress cannot exceed the yield stress and structural steels behave linearly below the yield stress, linear-elastic material model is sufficient. The FE model is depicted in Fig. 10.

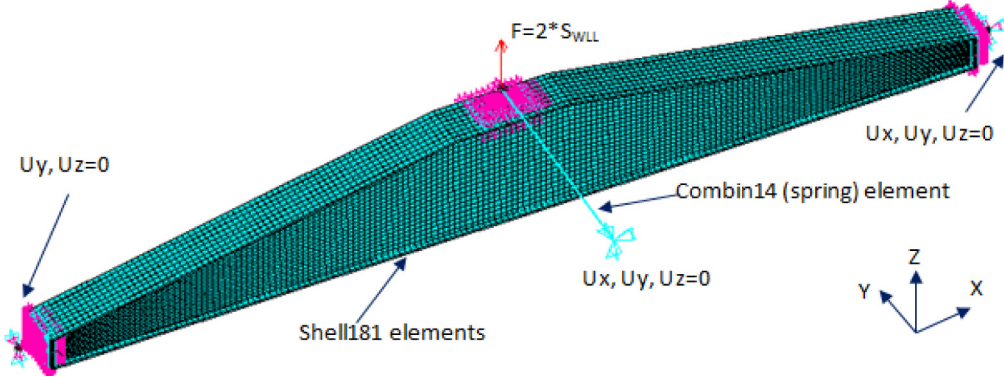


Fig. 10. FE model description

4.5. FE analyses

Three kinds of FE analyses are carried out at each design point:

- **Linear buckling analysis (LBA)**

This analysis is used to calculate the lowest critical buckling load. In addition, the lowest local buckling shape is identified to be used as the accompanying imperfection in GNIA.

- **Linear elastic analysis (LEA)**

This analysis is used to generate the geometric stiffness matrix \mathbf{K}_G for LBA and to develop the global (flexural-torsional) imperfection shape to be used in GNIA. This is accomplished by applying a continuously distributed lateral load to the bottom flange in order to generate lateral deflection of the bottom flange and cross section rotation.

- **Geometrically nonlinear elastic analysis with imperfections (GNIA)**

The resulting pattern of equivalent geometric imperfections is introduced to the FE model by scaling and superimposing mode shapes of the leading and accompanying imperfections. The amplitudes are given in Table C.2 of [3]. The global (lateral-torsional) imperfection amplitude is given as

$$e_{LT} = 0.5 \cdot L/150 [\text{mm}], \quad (24)$$

where L is the beam length. For the amplitude of the global imperfection, Table C.2 of [3] makes reference to Table 5.1 of [2]. Based on the buckling curve d (given by Table 6.4 of [2]), an amplitude $L/150$ is considered. For lateral-torsional buckling, section 5.3.4(3) of [2] is applicable as well. The recommended value of factor $k = 0.5$ is used. The local imperfection amplitude is given as

$$e_{LB} = 0.7 \cdot b/200 [\text{mm}], \quad (25)$$

where b is the web height. The coefficient 0.7 is recommended in annex C of [3] for accompanying imperfections. The scaling and superimposing operations are practically performed by calling the UPGEOM command in Ansys. The imperfect beam is then incrementally loaded at least until the first yield is reached. In order to achieve better convergence, displacement-based loading is used. Since our design space does not allow extremely slender sections to be generated, the first yield criterion governs the design. Fig. 11 shows load-deflection diagrams of the optimal section. The load causing the first yield is indicated.

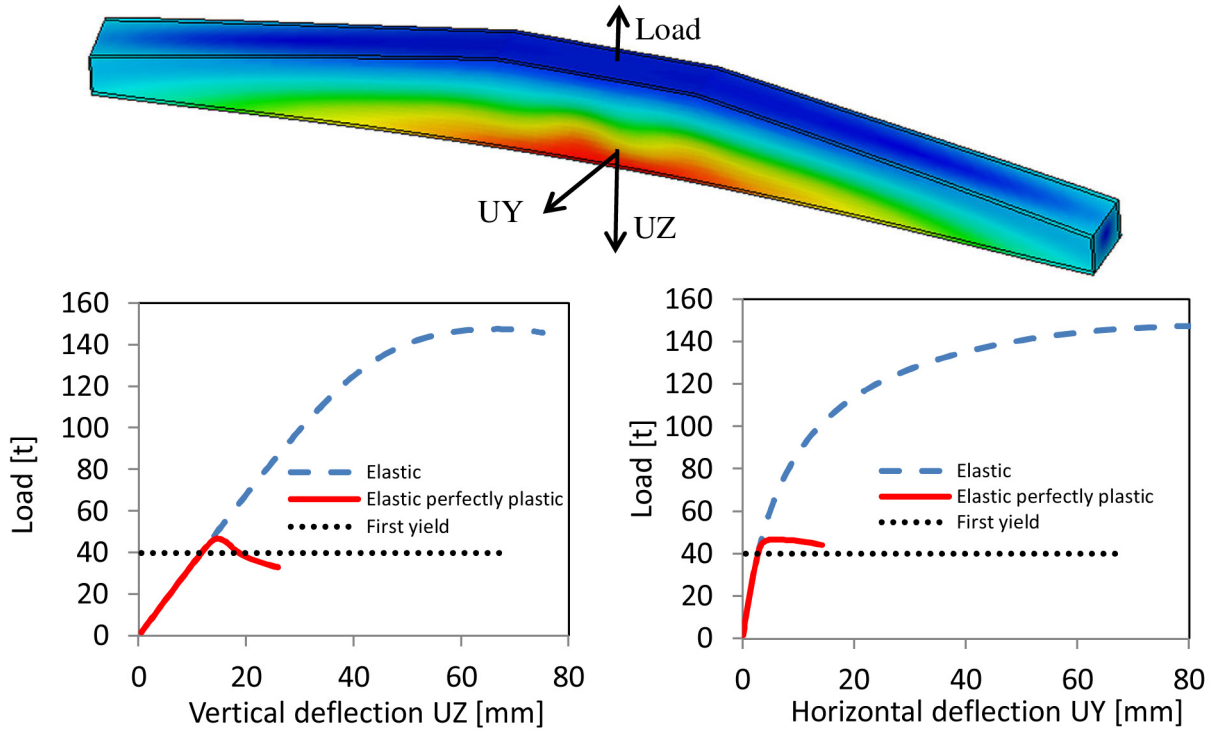


Fig. 11. Load-deflection diagrams of configuration: $tf = 8 \text{ mm}$, $tw = 4 \text{ mm}$

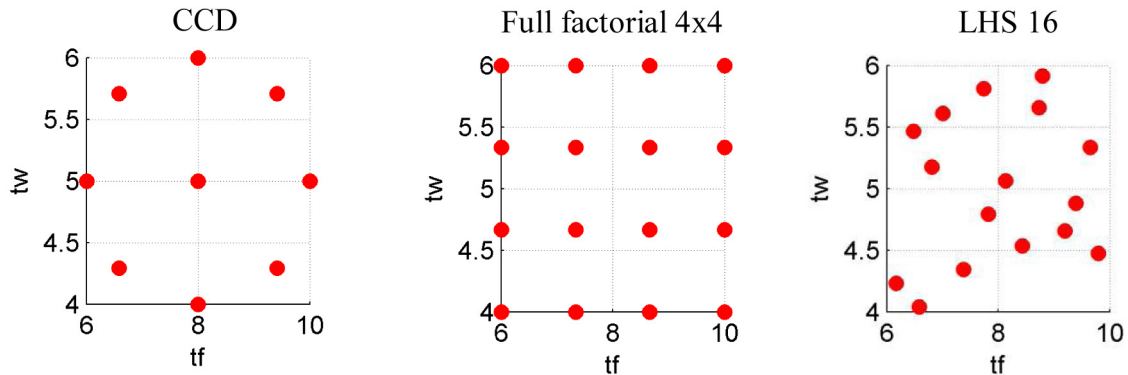


Fig. 12. Sampling plans in design space (tw and tf are in mm)

4.6. Design of experiments

Three sampling plans with different characteristics are used for comparison of resulting metamodels and optima. The sampling plans are listed below and depicted in Fig. 12.

- CCD is the most popular plan used to build quadratic polynomial metamodels. The number of samples generated by the CCD is given by the number of design variables.
- Full factorial design generates a regular grid of samples. Sixteen samples are generated in order to adequately and economically cover whole surface of the design space.
- LHS represents the space filling plans. The basic variant with sixteen samples is used.

The parametric FE model was executed for all DOE sample points and all required responses were calculated. Because of the amount of data, Table 2 lists the calculated values for the full factorial design only.

Table 2. Calculated data – full factorial design

| design point | flange thickness (tf) [mm] | web thickness (tw) [mm] | vertical deflection (δ) [mm] | equivalent stress (σ_{EQV}) [MPa] | buckling safety factor (k_B) [-] | beam volume [mm ³] |
|--------------|--------------------------------|-----------------------------|---------------------------------------|--|--------------------------------------|--------------------------------|
| 1 | 6.0 | 4.7 | 6.9 | 475 | 1.3 | 24 843 646 |
| 2 | 7.3 | 4.0 | 6.2 | 390 | 1.6 | 27 662 164 |
| 3 | 8.7 | 4.0 | 5.4 | 338 | 1.9 | 30 480 893 |
| 4 | 10.0 | 4.0 | 4.9 | 294 | 2.1 | 33 299 410 |
| 5 | 6.0 | 4.7 | 6.5 | 437 | 1.7 | 26 870 414 |
| 6 | 7.3 | 4.7 | 5.9 | 360 | 2.2 | 29 688 932 |
| 7 | 8.7 | 4.7 | 5.2 | 307 | 2.6 | 32 507 661 |
| 8 | 10.0 | 4.7 | 4.7 | 282 | 2.9 | 35 326 178 |
| 9 | 6.0 | 5.3 | 6.1 | 405 | 2.1 | 28 896 878 |
| 10 | 7.3 | 5.3 | 5.7 | 313 | 2.8 | 31 715 396 |
| 11 | 8.7 | 5.3 | 5.0 | 288 | 3.3 | 34 534 125 |
| 12 | 10.0 | 5.3 | 4.5 | 260 | 3.9 | 37 352 642 |
| 13 | 6.0 | 6.0 | 6.5 | 369 | 2.6 | 30 923 646 |
| 14 | 7.3 | 6.0 | 5.5 | 294 | 3.4 | 33 742 164 |
| 15 | 8.7 | 6.0 | 4.9 | 264 | 4.1 | 36 560 893 |
| 16 | 10.0 | 6.0 | 4.3 | 246 | 4.9 | 39 379 410 |

Note: Vertical deflection is evaluated for the working load limit of 20 tons (196 200 N).

4.7. Identification of metamodel parameters

The objective function (18) and design constraints (1) through (3) are represented by quadratic polynomial metamodels in two dimensions. Equation (6) represents a general formula for this metamodel. Two-dimensional realization of equation (6) is given as

$$\hat{Y}(\mathbf{X}) = \beta_0 + \beta_1 \cdot tf + \beta_2 \cdot tw + \beta_3 \cdot tf^2 + \beta_4 \cdot tw^2 + \beta_5 \cdot tf \cdot tw, \quad (26)$$

where $\hat{Y}(\mathbf{X})$ is the metamodel, \mathbf{X} is the two-dimensional design vector given by (17), β_i is the i^{th} regression coefficient, tf and tw are design variables. The parameters are identified using REGRESS function in Matlab. The metamodel parameters for all three sampling plans are listed in Table 3 and the goodness of fit measures are listed in Table 4. The resulting metamodels for the full factorial design are depicted in Fig. 13. The goodness of fit assessment as well as the graphical representation of metamodels in Fig. 13 confirms good approximation of the FE data by the second order polynomials metamodel.

4.8. Mathematical optimization

Both SQP and GA are realized in the optimization toolbox of Matlab (release 2011a). The SQP is implemented in the *fmincon* solver and the GA in the *ga* solver. The *fmincon* and *ga* solvers are configured by changing properties of *optimset* and *gaoptimset* structures, respectively. The *fmincon* solver was configured to start from the middle of design space. Finding adequate tolerances on constraints (*Tolcon*) and on cumulative change in the objective function value (*Tolfun*) is quite cumbersome, because these tolerances are relative. Since the runtimes of both

Table 3. Metamodel parameters

| DOE plan | metamodel | β_0 | β_1 | β_2 | β_3 | β_4 | β_5 |
|---------------|---------------------------|-----------|-----------|-----------|-----------|-----------|-----------|
| CCD | σ_{EQV} [MPa] | 1 431.0 | -188.9 | -46.7 | 13.7 | 5.4 | -10.2 |
| | δ [mm] | 16.4 | -1.3 | -1.5 | 0.0 | 0.0 | 0.1 |
| | k_B [-] | 4.0 | -0.4 | -1.5 | 0.2 | 0.0 | 0.1 |
| | Volume [mm ³] | 164 | 2 113 930 | 3 039 983 | 0 | 0 | 0 |
| Full 4 × 4 | σ_{EQV} [MPa] | 1 651.0 | -193.3 | -125.1 | 7.3 | 7.5 | 2.6 |
| | δ [mm] | 15.5 | -0.8 | -1.7 | 0.0 | 0.0 | 0.1 |
| | k_B [-] | 2.6 | -0.3 | -1.0 | 0.2 | 0.0 | 0.1 |
| | Volume [mm ³] | 59 | 2 113 954 | 3 039 970 | 0 | 0 | 0 |
| LHS 16 | σ_{EQV} [MPa] | 1 738.3 | -216.4 | -133.9 | 11.8 | 7.7 | 0.5 |
| | δ [mm] | 19.2 | -0.6 | -3.6 | 0.0 | 0.0 | 0.3 |
| | k_B [-] | 2.3 | -0.2 | -1.1 | 0.2 | 0.0 | 0.0 |
| | Volume [mm ³] | -1 631 | 2 113 771 | 3 040 903 | 84 | -14 | -157 |

Table 4. Goodness of fit assessment

| DOE plan | metamodel | R^2 | Adj^2 | REL | MAX |
|---------------|---------------------------|-------|---------|-------|--------|
| CCD | σ_{EQV} [MPa] | 1.00 | 0.99 | 1.7 % | 6.07 |
| | δ [mm] | 0.98 | 0.95 | 2.4 % | 0.14 |
| | k_B [-] | 1.00 | 1.00 | 1.0 % | 0.03 |
| | Volume [mm ³] | 1.00 | 1.00 | 0.0 % | 24.82 |
| Full 4 × 4 | σ_{EQV} [MPa] | 0.99 | 0.99 | 4.8 % | 14.95 |
| | δ [mm] | 0.99 | 0.98 | 3.6 % | 0.22 |
| | k_B [-] | 1.00 | 1.00 | 2.0 % | 0.06 |
| | Volume [mm ³] | 1.00 | 1.00 | 0.0 % | 154.65 |
| LHS 16 | σ_{EQV} [MPa] | 0.99 | 0.98 | 4.2 % | 13.08 |
| | δ [mm] | 0.99 | 0.99 | 2.7 % | 0.16 |
| | k_B [-] | 1.00 | 1.00 | 1.5 % | 0.04 |
| | Volume [mm ³] | 1.00 | 1.00 | 0.0 % | 172.87 |

solvers were quite short, tight tolerances were used. The size of population of the *ga* solver was increased to 600 and the crossover fraction was set to 0.7 in order to ensure that the individuals in each new generation are densely spread through the whole area of design space, thereby making the convergence faster. The maximum number of generations was limited to 100. The solver was also set to stop, if there was no improvement in the objective function for 10 subsequent generations. Configurations of both solvers are summarized in Table 5. The properties which are not listed used their defaults.

The calculated optima are listed in Table 6 and graphically depicted in Fig. 14 for metamodels based on all considered DOE plans. Since the objective function and design constraints are represented by smooth second order polynomials with low degree of curvature (see Fig. 13) it was possible to configure both solvers so that identical optima were achieved in reasonable time. Getting identical optima from both solvers proves their correct adjustment. Regarding results, we have to realize that the plate thicknesses are modelled as continuous variables although they

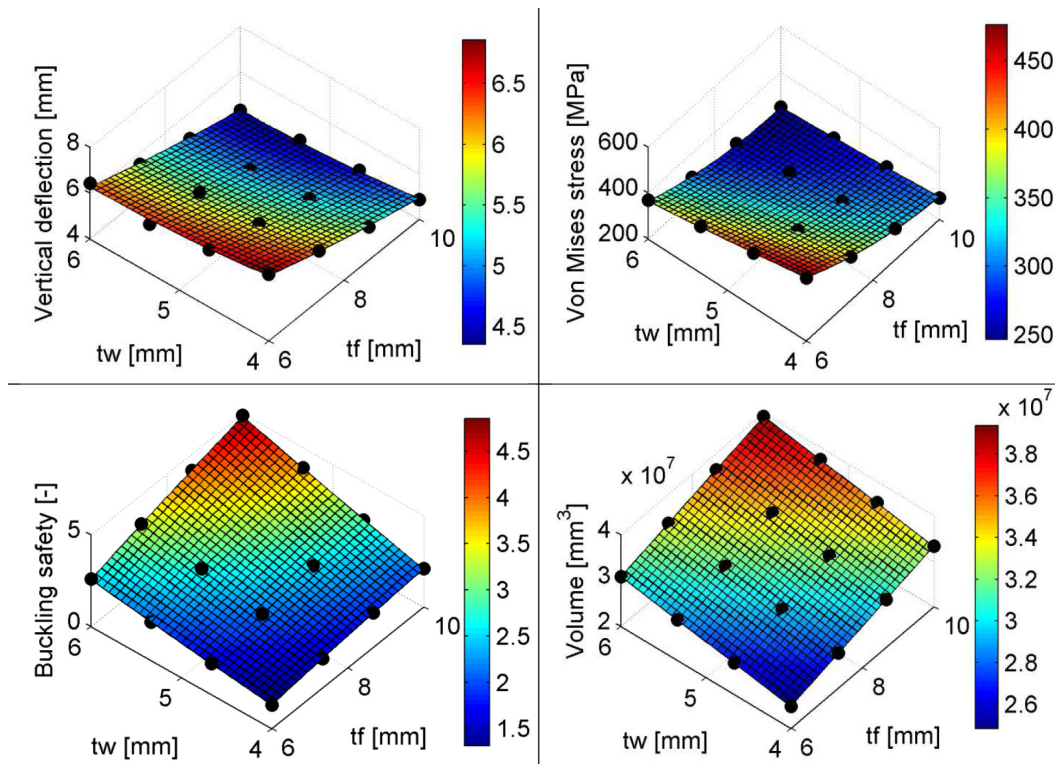


Fig. 13. Metamodels based on the full factorial design

Table 5. Configuration of optimization algorithms in Matlab

| SQP | | GA | |
|-----------|------------------------|-------------------|------------------------|
| Property | Value | Property | Value |
| solver | fmincon | solver | ga |
| algorithm | sqp | Tolcon | 1e-9 |
| Tolcon | 1e-9 | Tolfun | 1e-9 |
| Tolfun | 1e-9 | MutationFcn | @mutationadaptfeasible |
| x_0 | middle of design space | PopulationSize | 600 |
| | | PopInitRange | whole design space |
| | | CrossoverFraction | 0.7 |
| | | Generations | 100 |
| | | StallGenLimit | 10 |

Table 6. Calculated optima

| Sampling plan | Optimization algorithm | tf [mm] | tw [mm] |
|---------------|------------------------|-----------|-----------|
| CCD | SQP | 8.0 | 4.0 |
| | GA | 8.0 | 4.0 |
| Full 4 × 4 | SQP | 8.1 | 4.0 |
| | GA | 8.1 | 4.0 |
| LHS 16 | SQP | 7.9 | 4.0 |
| | GA | 7.9 | 4.0 |

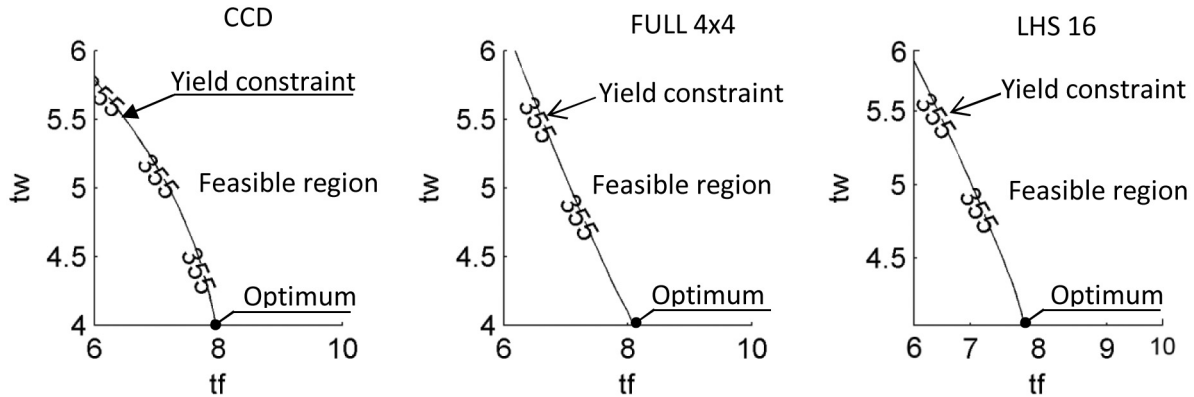


Fig. 14. Constraints and optima in design space

are discrete in reality; therefore, the optimum has to be rounded to commercially available plate thicknesses. Considering available plate thicknesses as 4, 5, 6, 8 and 10 mm, the practically realizable optimal configuration is: $tf = 8$ mm and $tw = 4$ mm. Moreover, we have to keep in mind that the optimum configuration was calculated by using metamodels (i.e., approximations of FE simulations, which possess bias errors); therefore they cannot be necessarily feasible in reality and have to be verified by FE calculation. Table 7 lists responses of metamodels in optimum points from Table 6 and Table 8 lists the calculated responses in the proposed optimum configuration.

Table 7. Metamodel responses in optima

| response | CCD approx. | Full 4×4 approx. | LHS 16 approx. |
|--------------------------|-------------|---------------------------|----------------|
| σ_{EQV} [MPa] | 355 | 355 | 355 |
| δ [mm] | 5.8 | 5.8 | 6.1 |
| k_B [-] | 1.8 | 1.8 | 1.7 |
| volume [mm^3] | 28 991 296 | 29 222 152 | 28 813 206 |
| weight [kg] | 228 | 229 | 226 |

Note: weight is calculated from volume considering steel density $\varrho = 7.85 \times 10^{-6}$ kg/mm³

Table 8. Verification of optimum responses

| response | $tf = 8$ $tw = 4$ |
|--------------------------|----------------------|
| σ_{EQV} [MPa] | 353 |
| δ [mm] | 5.8 |
| k_B [-] | 1.8 |
| volume [mm^3] | 29 071 528 |
| weight [kg] | 228 |

Note: weight is calculated from volume considering steel density $\varrho = 7.85 \times 10^{-6}$ kg/mm³

5. Conclusion

This paper provided an overview of the metamodel-based optimization approach along with specific recommendations for plated beams. Special attention was paid to the stability analysis.

To account for the detrimental influence of imperfections on the limit load, the concept of equivalent geometrical imperfections from EC3 was adopted. Because of the lack of data in the design stage, using this concept is the best what an analyst can do.

The practical part illustrated the metamodel-based optimization process on the step by step basis. Metamodels from different DOE plans were constructed and subsequently used by two principally different optimization algorithms. Identical optima from both algorithms confirmed correct adjustments. The *ga* solver had to work with large populations, thereby its runtime was approximately twenty times longer than the runtime of *fmincon* solver, but it was negligible in comparison to runtimes of nonlinear analyses in Ansys.

Regarding the optimization results, we can say that the metamodels from different DOE plans and the corresponding optima are nearly identical. This can be attributed to small design space and low variance of responses in this design space. Since this is not general case, analysts should be aware of approximate character of metamodeling and properly review and verify results. In our case, the practically realizable optimum was easy to find because of rounding to commercially available plate thicknesses.

Modelling of discrete variables as continuous is quite common, because continuous functions provide better understanding of relationships between design variables and responses. Furthermore, optimization of plated structures often includes both continuous (dimensions) and discrete (thicknesses) variables.

It is common practice to use stiffeners to prevent local buckling and thereby achieving better weight/strength ratios. Due to high cost of manpower required for welding, stiffeners are often eliminated and thicker plates are used. The decision on using stiffeners depends on preferences of the particular application. The lowest weights/strength ratio is generally achieved by adequate stiffening, even though the cost is higher. The described methodology can be applied to stiffened beams as well.

The future research is focused on application of metamodel-based optimization to fatigue criteria. Here, the second order polynomial metamodels do not seem to work well due to high nonlinearity and variability in the fatigue usage. The problem is also complicated by the fact that structural standards use different fatigue curves for different design details.

Reference

- [1] ČSN EN 13155+A2, Cranes-Safety-Non-fixed load lifting attachments, Czech Office for Standards Metrology and Testing, 2009, (in Czech).
- [2] ČSN EN 1993-1-1, Eurocode 3: Design of steel structures – Part 1-1: General rules and rules for buildings, Czech Office for Standards Metrology and Testing, 2006, (in Czech).
- [3] ČSN EN 1993-1-5, Eurocode 3: Design of steel structures – Part 1-5: Plated structural elements, 2nd edition, Czech Office for Standards Metrology and Testing, 2013, (in Czech).
- [4] ECCS, Buckling of steel shells-European design recommendations, 5th edition, 2008.
- [5] Galambos, T., Guide to stability design criteria for metal structures, 5th edition, New York, John Wiley, 1998.
- [6] Giunta, A. A., Wojtkiewicz, S. F. Jr., Eldred, M. S., Overview of modern design of experiments methods for computational simulations, 41st AIAA Aerospace Sciences Meeting and Exhibit, 2003.
- [7] Montgomery, D. C., Design and analysis of experiments, 8th edition, John Wiley & Sons, 201.
- [8] Nocedal, J., Wright, S. J., Numerical optimization, 2nd edition, Springer Series in Operations Research, Springer Verlag, 2006.
- [9] Rao, S. S., Engineering optimization: Theory and practice, 4rd edition, John Wiley & Sons, 2009.